THE GEOLOGICAL SOCIETY OF AMERICA®

Lineaments and earthquake ruptures on the East Japan megathrust

Gordon Lister[1]*, Hrvoje Tkalčić[1], Babak Hejrani[1], Achraf Koulali[1], Eelco Rohling[1,2], Marnie Forster[1], and Simon McClusky[1]
[1]RESEARCH SCHOOL OF EARTH SCIENCES, AUSTRALIAN NATIONAL UNIVERSITY, CANBERRA 2601 AUSTRALIA
[2]OCEAN AND EARTH SCIENCE, UNIVERSITY OF SOUTHAMPTON, NATIONAL OCEANOGRAPHY CENTRE SOUTHAMPTON, SO14 3ZH, UNITED KINGDOM

ABSTRACT

In this paper we describe the earthquake geology of East Japan, based on a seismotectonic analysis of foreshocks and aftershocks for the 2011 Tohoku-oki Great Earthquake. The earthquake geology is defined by three compressional buttresses that are separated by channels dominated by extensional earthquakes. In the 2011 earthquake sequence, most activity occurred in the Tohoku-oki extensional channel. This is bounded by seismotectonic lineaments that run subparallel to the slip direction of thrust-fault earthquakes in the adjacent compressional buttresses, and to the slip direction of landward-dipping normal-fault aftershocks in the subducting Pacific plate. The northern bounding seismotectonic lineament of the Tohoku-oki extensional channel runs WNW-ESE ~15 km north of the Miyagi Volcanic Lineament. The southern bounding seismotectonic lineament runs ~20 km to the south of the Fukushima Volcanic Lineament. These lineaments may reflect faults that splay from deeper structures beneath the volcanic lineaments. In any case, the seismotectonic lineaments appear to reflect zones of weakness, and as is the case in any load-bearing architecture, precursor movements on such focusing structures may herald the onset of catastrophic failure. We discovered that two-thirds of all major earthquakes with moment magnitude $M_w \geq 6.9$ in the past 40 years in East Japan began within 15 km of the seaward prolongation of a volcanic lineament, and that motion across the northern seismotectonic lineament reversed its sense in the days prior to the 2011 Great Earthquake, suggesting the onset of yield. We infer that continuous geodetic monitoring across the East Japan lineaments might thus provide useful signals for future hazard assessment.

LITHOSPHERE; v. 10; no. 4; p. 512–522; GSA Data Repository Item 2018143 | Published online 18 April 2018 https://doi.org/10.1130/L687.1

INTRODUCTION

There is a continuing debate as to whether science will ever allow prediction as to when and where earthquakes initiate. To make progress, we need to better understand how load is distributed during the build-up of tectonic stress prior to catastrophic failure, and how the complex material properties of rock affect the outcome. It is also important that we determine how geological structures in the loaded region influence where and when yield commences at the start of an earthquake, in map view (Bassett et al., 2016; Ikeda et al., 2009) as well as in three dimensions (Lister et al., 2008). This is difficult, because the way stress accumulates during loading is influenced by the natural heterogeneity and variable mechanical properties of rock. Nevertheless, the tectonic architecture is critical, and we need to determine its influence.

Just as an engineer will study the structure around a dam that has failed, to assess whether there were specific weaknesses that predicated that outcome, a geoscientist can forensically examine the structure of a region that has hosted a large earthquake. We can thus seek to determine whether controlling structures exist that localized the onset of failure, and if such focusing structures might have been monitored to allow accelerating precursor motion to be detected in the weeks, months, years, or even decades prior to a catastrophic event. In this paper, we report the outcome of such a forensic analysis for the earthquake geology of the 2011 Tohoku-oki Great Earthquake on the East Japan megathrust.

There have been few attempts at seismotectonic analysis at map scale. Nakajima et al. (2009) provide an in-depth analysis of the Tokyo region, and provide important data on slab geometry. Otherwise, research on this topic has focused on the seismic potential of different domains (e.g., Triyoso and Shimazaki, 2012), with a multivariate statistical approach adopted by Kumamoto et al. (2016) allowing a revision focused on moment magnitude. Ghimire and Kasahara (2009) focus on stress analysis, linking regional stress axes to P-axis orientation during earthquake moment release, but this analysis did not account for fault kinematics. Kyriakopoulos et al. (2013) use finite element models to examine heterogeneities in the margin architecture. Sato et al. (2013) examine the seismotectonic architecture from the point of view of the location of high-slip patches. Zhao et al. (2011) consider structural heterogeneity of the megathrust and the 2011 earthquake mechanism. The approach adopted here is outlined in Lister et al. (2014), and in Lister and Forster (2018), who applied similar methods to seismotectonic analysis of the significance of fault movements during the 2004 Great Earthquake in the Andaman Sea.

SEISMOTECTONIC ANALYSIS

We began with data from the Global Centroid-Moment-Tensor (CMT) Project (Ekström et al., 2012; Nettles et al., 2011). This catalogue includes

Gordon Lister http://orcid.org/0000-0001-6265-602X

the strike, dip, and rake of two possible but conjugate fault planes for many earthquakes. These conjugate solutions are characterized by a simple geometric relation: the slip line on one fault plane is orthogonal to the fault plane of the other. Because the sense of relative displacement for one conjugate fault plane solution is opposite to the sense of relative displacement for the other, the type classification of the fault geometry in all but a small minority of cases is the same for both solutions, even though the possible (conjugate) fault planes dip oppositely at ninety degrees to each other. This geometry is made evident in a beachball representation of the centroid moment tensor, with the shaded area defining the orientations of ray paths for compressional moment pulses emanating from the rupture. This geometry also makes it possible to automatically classify the type of rupture associated with an individual earthquake, here using the eQuakes program to characterize earthquake type.

The eQuakes program allows ready analysis of the geometry of earthquakes (Lister et al., 2014; Lister and Forster, 2018) and thus allows recognition of patterns in the type of faulting taking place during an earthquake sequence. Figure 1A shows epicenters for reverse faults and thrusts (red), normal faults (light blue), and strike-slip faults (purple). The classic beachball representation is also possible, but statistical analysis of the significance of orientation clusters can best be accomplished by grouping earthquakes and plotting slip line directions and fault plane normals in a scatter diagram, using the lower hemisphere of a stereographic projection.

To allow such statistical analysis, we constructed stereograms for slip lines and fault plane poles in the different spatial clusters that can be recognized (Figs. 1B–1H). We chose to do this for three months prior, and nine months after the 2011 Tohoku-oki Great Earthquake (Fig. 1A), to include foreshocks, and to limit earthquakes to those occurring immediately after the main rupture. In this way, we limit the seismotectonic analysis to consider only the geodynamic state of the lithosphere immediately prior to the main rupture, and during the early to mid-stages of the aftershock sequence. Initially, epicenters for all earthquakes with moment magnitude $M_w > 5$ were plotted, since these are more accurately located, and centroid moment tensor data is available.

The depth of the hypocenters analyzed was limited to <30 km, to allow a focus on crustal architecture. This cut-off depth was chosen because it encompasses the brittle-to-ductile transition in most crustal rocks, and thus includes almost all crustal seismicity in Japan. This choice of depth cut-off allows inclusion of all seismic activity associated with operation of the East Japan megathrust except that which occurs in the deep crust, and thus a focus on seismic activity in the down-going slab at its shallowest levels. Seaward of the megathrust, this choice of depth allows the geometry of normal fault earthquakes to be highlighted in the depth range that includes their most energetic seismogenic behavior. The Japanese lithosphere is ~70 km thick (Kanamori and Press, 1970).

In almost all cases, the inherent geometrical ambiguity present in focal plane solutions could be resolved by bringing geology into the equation (Lister et al., 2008, 2014; Lister and Forster, 2018). Earthquakes that result from normal faults (Jackson, 1987) typically have a slip line that plunges at ~60°, whereas classification of the fault plane normal and associated slip line for thrust faults can assume that the fault plane dips gently. In addition, for specific spatial groups of earthquakes, there are well-defined maxima on the scatter plot of earthquake slip lines and fault plane poles, so the faults causing these earthquakes are similarly oriented. This allowed ready classification of fault planes and slip line directions in orientation groups involving thrusts (Figs. 1B, 1C, and 1G) or normal faults (Figs. 1D, 1E, and 1F). It was also possible to resolve ambiguity for strike-slip fault solutions, by computing hypocenters and centroids for individual earthquakes using the Hypocenter-Centroid (H-C) method (Zahradník et al., 2005, 2008; Hejrani et al., 2010). This H-C method allowed classification of fault plane pole and slip line orientation clusters based on the fault plane solution that allows the alignment of the earthquake hypocenter and centroid in the same plane. The classification of fault geometry is shown on individual stereoplots.

SEISMOTECTONIC SEGMENTATION OF DEFORMATION MODE IN THE CRUST ABOVE THE MEGATHRUST

Typically, a high degree of kinematic coordination is observed in movements associated with particular spatial clusters of earthquakes (Lister et al., 2014; Lister and Forster, 2018). This patterning is responsible for the orientation clusters on lower hemisphere stereographic projections when slip lines and/or fault plane poles are plotted for individual spatial clusters (Fig. 1). Such an analysis makes it obvious that there was a distinct and marked segmentation of tectonic modes above the megathrust. There are three spatial clusters of thrust earthquakes offshore East Japan (red circles in Fig. 1A). These each have a well-defined orientation group evident in the corresponding scatter plot (Figs. 1B, 1C, and 1G), and we thus infer similarly oriented principal compressive stress axes. Assuming Coulomb-Mohr failure, these three segments were subject to horizontal, margin-orthogonal shortening, and thus acted as compressional buttresses ramming the subducting Pacific Plate.

The compressional buttresses (Fig. 1) are named in turn: (*i*) the Sanriku buttress, with thrust faults that dip ~20° toward the WNW, and slip directions trending ~110° (shown in the scatter plot, Fig. 1B); (*ii*) the Tohoku-oki buttress, again with thrust faults that dip ~20° toward the WNW, and slip directions that trend ~110° (shown in the scatter plot, Fig. 1C); and (*iii*) the Joban buttress, with thrust faults that dip ~25° toward the WNW, and slip directions trending ~115° (again shown in a scatter plot, Fig. 1G).

There are prominent volcanic lineaments in East Japan (Fig. 2), and it is of interest that these approximate the seismotectonic bounds of the compressional buttresses. Most seismic activity in the Sanriku buttress is bounded to the north by the Aomori Volcanic Lineament and to the south by the Sanriku Volcanic Lineament. Similarly, the Tohoku-oki buttress is bounded to the north by the Chokai Volcanic Lineament, while to the south it is bounded by a seismotectonic lineament ~15 km to the north of the Miyagi Volcanic Lineament. The Joban buttress is bounded to the north by a seismotectonic lineament ~20 km south of the Fukushima Volcanic Lineament, and to the south by the Haruna Volcanic Lineament.

Between the three compressional buttresses are "channels" in which normal-fault earthquakes dominated, implying margin orthogonal extension (Fig. 1). These channels are of particular interest for several reasons, as will be outlined in the remainder of the paper. The channels are: (*i*) the Tohoku-oki channel (which was the most active during the 2011 earthquake); and (*ii*) the Sanriku channel. Here we focus on the Tohoku-oki channel, which encompasses two important volcanic lineaments: (*i*) the Miyagi Volcanic Lineament in its northern extent; and (*ii*) the Fukushima Volcanic Lineament in its southern extent. The coincidence between the bounding seismotectonic lineaments and the volcanic lineaments is not exact: there is an offset, as noted.

We can relate inferred segment boundaries on the megathrust to the pattern of movement implied by the foreshocks and earthquakes. The contoured scatter plots (Fig. 1) show that slip lines for foreshock thrust fault earthquakes are statistically parallel, and close to the ~NW-SE trend of the margins of the seismotectonic segments (Fig. 1). Each slip line marks the direction of relative movement on a fault rupture, shown using the relative motion of the hanging wall (or upper-plate) of the faulted rock mass. The trends of the slip lines are concentrated with an azimuth of 292–294°, a direction within a few degrees of the 286–287° trending volcanic lineaments that can be seen on land (Fig. 2). Symmetry requires

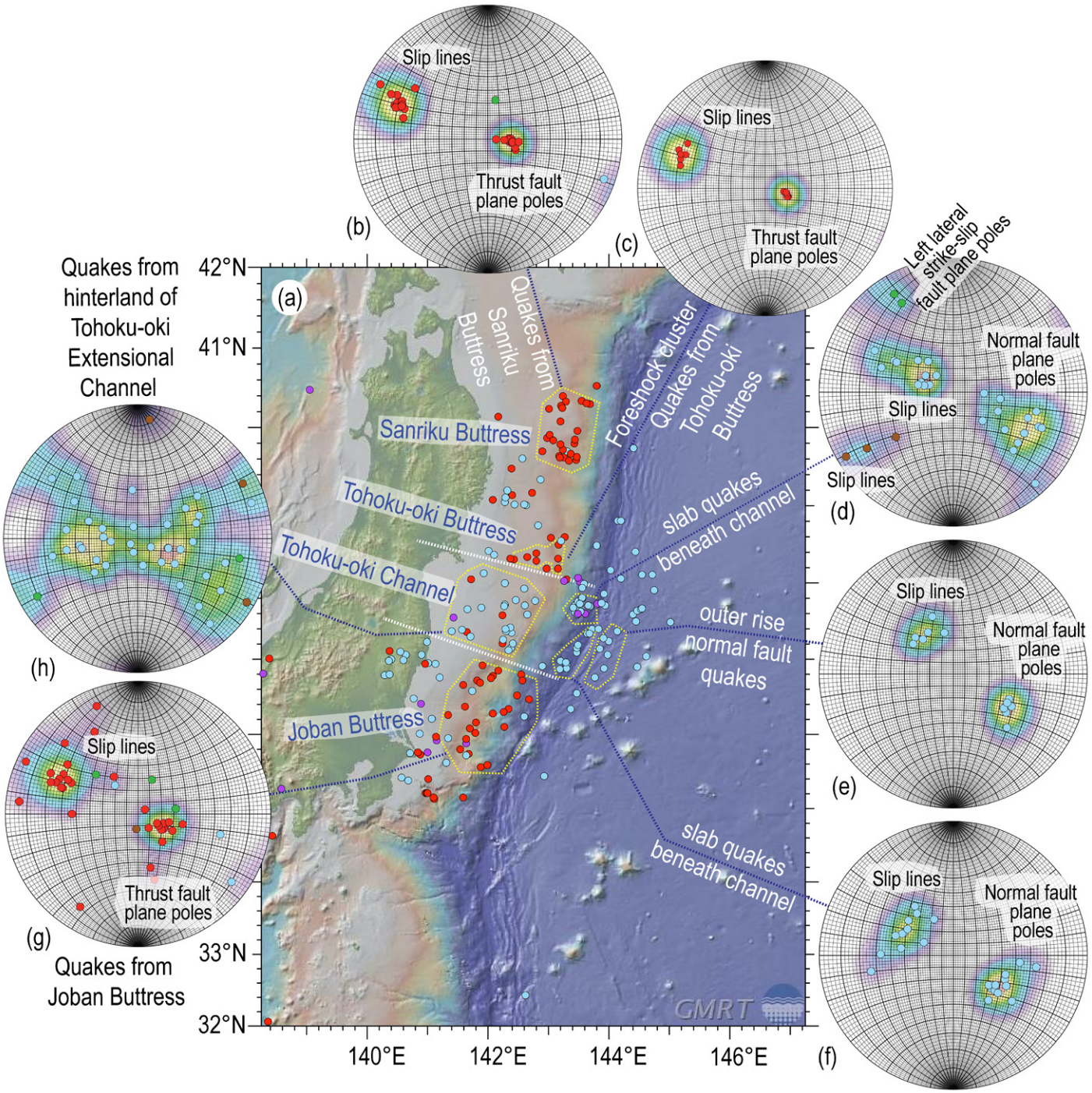

Figure 1. Epicenters (A) for all 2011 earthquakes in the Global CMT Project catalogue (Ekström et al., 2012; Nettles et al., 2011): blue circles—normal fault (extensional) earthquakes; red circles—thrust-fault (compressional) earthquakes; purple circles—strike-slip earthquakes. The Miyagi and Fukushima Lineaments bound an extensional channel, 120–130 km across. Fault plane poles and associated slip lines shown on stereoplots: (B) thrust faults in the Sanriku compressional buttress; (C) foreshock thrusts in the compressional buttress north of the extensional channel; (D, E, F) normal fault earthquakes in the upper levels of the down-going (subducting) Pacific Plate dip landward, as would be the case for Basin and Range style tilt blocks. (F) A cluster of left-lateral strike-slip fault earthquakes, parallel to the Median Tectonic Line; (G) thrust earthquakes mark the southern compressional buttress; (H) dominantly extensional earthquakes in the hinterland of the extensional flow channel, with poorly defined orientation groups. Data on a Mercator projection with the background image derived from the Global Multi-Resolution Topography Data Portal (Ryan et al., 2009).

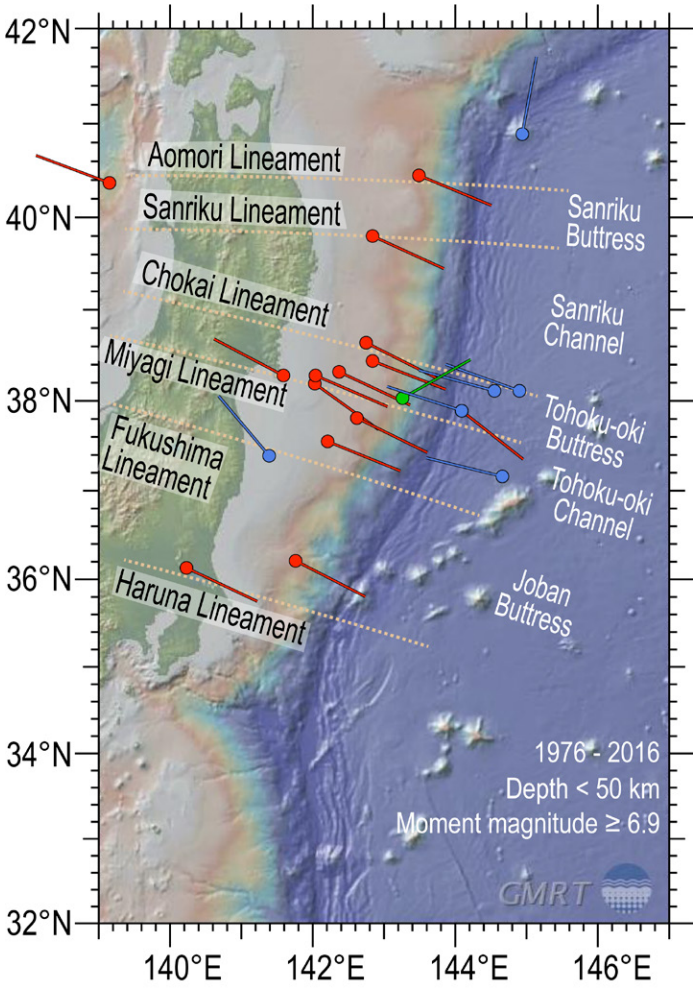

Figure 2. Epicenters for all events since 1976 with moment magnitude (M_w) >6.9, from the Global CMT Project catalogue (Ekström et al., 2012; Nettles et al., 2011) plotted on a Mercator projection with the background image derived from the Global Multi-Resolution Topography Data Portal (Ryan et al., 2009), and using program eQuakes to show the trend of slip line vectors. The volcanic lineaments were defined by great circles that showed a least-squares best fit to topographic highs (see Data Repository Item, footnote 1). The prolongations of these lineaments eastward may mark the locus of (weak therefore aseismic) crustal breaks that localize the onset of major earthquakes. The prolongation onto the Pacific Plate is justified in that there may be structural interactions as yet unknown, or localized stress variation controlled by the geodynamics of the adjacent segment of the marginal megathrust. It is evident that many of the large earthquakes fall on or close to these great circles.

that in the reverse fault segments the principal stress axis, σ_1, is subhorizontal, trending ~5° clockwise from the trend of the volcanic lineaments.

Prior to the 2011 Great Earthquake, a foreshock cluster of compressional thrusts occurred, limited to the narrow extent of the Tohoku-oki buttress (Fig. 1C). Compressional earthquakes also define the southern buttress to the extensional channel and mark another switch in tectonic mode, south of the Fukushima Lineament. Structures parallel to the bounding lineaments thus separate different types of earthquakes, and there are abrupt changes from margin-orthogonal compression to margin-orthogonal extension across them. It is important to understand how this might have been possible: e.g., why margin-orthogonal horizontal compression caused thrust fault earthquakes from ~20 km north of the Miyagi Lineament, while normal fault extensional earthquakes took place immediately to the south of this boundary.

It is also important to understand why normal fault earthquakes were prevalent in the subducting slab adjacent to the extensional earthquake channel. Such outer-rise earthquakes did continue northward, and southward, thus also forming seaward of the compressional buttresses, but occurred in markedly lower numbers in those regions. They concentrated in great number immediately adjacent to and in the slab beneath the crust in the Tohoku-oki extensional channel.

It is particularly significant that the fault plane appears to consistently dip landward for most of these normal-fault earthquakes (Figs. 1D, 1E, and 1F), so this aspect was examined in more detail. Their landward-dip was confirmed by more detailed analysis, as detailed in a subsequent section. In comparison, the hinterland of the extensional channel was marked by earthquakes on normal faults with scattered orientations (Fig. 1H). All normal faults in the hinterland of the extensional channel occurred in the top 30 km of the crust, above the megathrust as it shallows from ~40 km to its eventual outcrop in the trench. Thrust fault earthquakes are few in number and occur near the megathrust, at the base of the extensional channel. The thrust fault solutions are almost all associated with failure on fault planes that dip northwest, i.e., with fault planes that likely merge with and/or are parallel to and/or coincident with the main megathrust (Figs. 1B, 1C, and 1G).

There are some strike-slip earthquakes within the subducting slab. The H-C method applied to these earthquakes implies left-lateral strike-slip faulting in the surface levels of the subducting Pacific Slab, where it meets the Miyagi Lineament. The slip direction trends parallel to the Median Tectonic Line, supporting Bassett et al. (2016). Such earthquakes would occur in the subducting slab if there was movement prior to or during the aftershock sequence, implying the Japanese crust had indented the subducting Pacific Plate.

THE VOLCANIC LINEAMENTS OF EAST JAPAN

To further assess the role of the volcanic lineaments, we considered the coincidence of the seaward prolongations of their trends with earthquake epicenters (Fig. 2A). The lineament trajectories were defined using topographic images, selecting peaks and ridge lines (see File DR1 in the Data Repository Item[1]), defining for each point a position vector in 3-D Cartesian coordinates. The array of normalized position vectors for each lineament was contracted into a 3 × 3 orientation matrix, and the eigenvalues and eigenvectors of this matrix were then determined. The eigenvector orthogonal to the plane of best fit was used to determine how close any individual hypocenter was to an individual lineament. In all cases, the distance between the epicenter and the closest lineament was considered. This value was tabulated (Fig. 3) with the histograms showing the variation in distance of epicenters from the closest lineament, with moment magnitude cut-off at different values.

[1]GSA Data Repository Item 2018143 includes File DR1: Data used to generate the best fit to the topographic lineaments, and Table DR2: Centroid-moment-tensor solutions calculated in this study for 84 earthquakes. The data used to delineate lineaments are latitude-longitude locations on topographic highs along the lineament trend, selected from within the eQuakes program. These data are then used to construct a matrix of position vectors in Cartesian space, which is then contracted to a 3 × 3 orientation matrix. The eigenvector of the orientation matrix that corresponds to the smallest eigenvalue then defines the pole to the great circle that has the least-squares best fit along the lineation trend. The data repository item is available at http://www.geosociety.org/datarepository/2018, or on request from editing@geosociety.org.

Systematic recording of data in earthquake catalogues has yet to reach its first half century, so only the most seismically active regions have experienced enough large events to allow statistical analysis. We set an upper limit as $M_w \geq 6.9$ to ensure a significant number of major events could be analyzed, to recognize statistical trends. We found that almost two-thirds of the epicenters from the Global CMT Project database for earthquakes with moment magnitude $M_w \geq 6.9$, since 1976, began within 15 km of one of the volcanic lineaments (Fig. 3). These concentrations of epicenters remain visible at lower moment magnitude cut-off values, but the correlation is most marked for the largest magnitude earthquakes.

We must conclude that there are physical structures associated with the volcanic lineaments, and that these played a significant role in triggering, or localizing the onset of major earthquakes on the East Japan megathrust. The next question, therefore, concerns their physical expression and mechanical strength. One can imagine the existence of faults that remain steep and thus continue the trends of the volcanic lineaments to shallower levels, as well as faults that curve from deeper structures while remaining parallel to these trends. We can infer that these structures must be weak because earthquake rupture planes never parallel these trends.

MARGIN SEGMENTATION FROM PREVIOUS MECHANICAL MODELING AND SATELLITE GEODESY

Numerous previous studies show the value of combining the analysis of satellite geodesy with mechanical modeling (Ikuta et al., 2012; Kato et al., 2012; Ozawa et al., 2012; Kyriakopoulos et al., 2013; Mavrommatis et al., 2014, 2015; Hasegawa and Yoshida, 2015; Johnson et al., 2016; Loveless and Meade, 2016; Hashima and Sato, 2017; Yokota and Koketsu, 2015). Several of these works demonstrate patterns that suggest the existence of margin segments similar to those recognized by the seismotectonic results presented above. For example, Ozawa et al. (2012), Hashima and Sato (2017), and Perfettini and Avouac (2014) highlight interesting aspects in the context of the segmentation inferred in this paper: (*i*) maximum coseismic and post-seismic displacement focused in the offshore prolongation of the Tohoku-oki compressional buttress (Fig. 1); and (*ii*) vertical acceleration focused within the Tohoku-oki buttress and the northern edge of the Joban buttress. However, the most compelling comparison comes from Loveless and Meade (2016) in diagrams that plot velocity changes in a (Lagrangian) reference framework based on the pattern of movement in their Epoch I (from 1996 to 1999). Their figures 5b and 5c show the velocity changes in four-year intervals up to the time of the 2011 Great Earthquake. For eight years prior to the main rupture, the Sanriku buttress accelerated westward (so material points were driven with ever increasing velocity away from the trench), in a direction roughly parallel to the Sanriku volcanic lineament. For the segments southward up until the southern margin of the Tohoku-oki buttress, as defined by the seismotectonic segmentation shown in Figure 1, there is little change in velocity. Southward of the Tohoku-oki buttress, however, for the eight years prior to the main rupture, the margin segment we refer to here as the Tohoku-oki extensional aftershock channel accelerated toward the southeast, or east-southeast (i.e., against the WNW-directed movement defined by Epoch I).

These observations are consistent with the conclusion that the buttresses focused loading during the decades prior to the Great Earthquake. Further, since the foreshocks to the Tohoku-oki Great Earthquake took place exclusively within the Tohoku-oki buttress, the southern margin of the Tohoku-oki buttress can be argued to have focused the accumulation of deviatoric stress. The foreshocks involved displacement on gently dipping thrusts (Ozawa et al., 2012; Sato et al., 2013) and can be taken as the first sign of imminent yield. This was registered by a reversal in the sense-of-shear across the buttress lineament, i.e., from left-lateral strike-slip in the eight years preceding failure, to right-lateral strike-slip in the time of precursor movements, and during the main rupture (Kamiyama et al., 2016). Later aftershocks within the northern reaches of the Joban buttress were also gently dipping thrust displacements, which explains the pattern of vertical uplift focused in or at the margins of the compressional buttresses. In contrast, extensional normal faulting at the seaward margin of the Tohoku-oki extensional channel requires either subsidence, or minimal vertical uplift, as observed (Hashima and Sato, 2017).

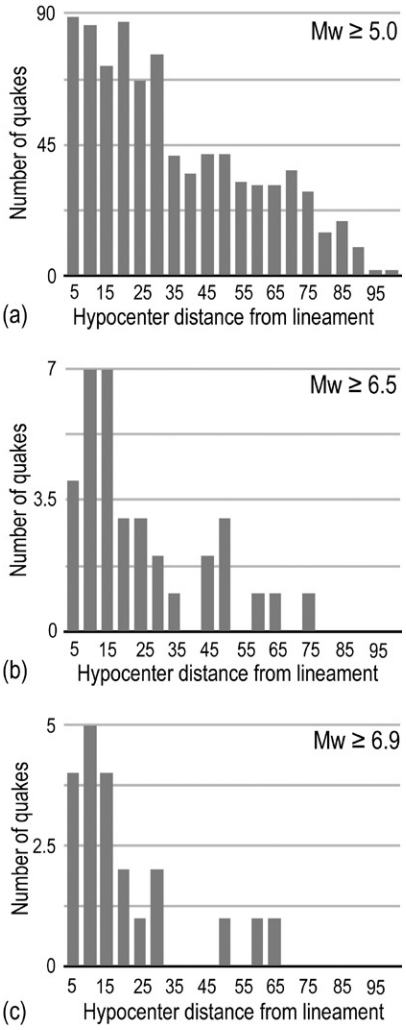

Figure 3. The histograms show the number of epicenters plotted against their distance from the closest lineament prolongation, with a 5 km bin size. An epicenter located 2 km from the closest great circle would plot in the column labeled 5 km, for example. The histograms are constructed for moment magnitude earthquakes $M_w \geq 5$ (A), $M_w \geq 6.5$ (B) and $M_w \geq 6.9$ (C). To give an idea as to the separation distance of individual great circles, the Chokai Lineament is ~70 km from the Miyagi Lineament, and the Miyagi Lineament is ~130 km from the Fukushima Lineament. The most recent large earthquake was a normal fault (M_w 6.9) event on 26 November 2016 with a rupture that ran northward from the seaward prolongation of the Fukushima Lineament.

The decadal signal showing landward acceleration of the Sanriku buttress (Loveless and Meade, 2016; Mavrommatis et al., 2015) can be interpreted as an effect caused by strain-hardening on the megathrust. Preliminary modeling we conducted shows that the effect can also result from increasing the down-dip extent of the locked area of the megathrust. Conversely, the seaward acceleration of the Tohoku-oki extensional channel to the south documented by Loveless and Meade (2016) can also result from decrease in the down-dip extent of the locked area of the megathrust. The switch in geodynamic behavior requires local increases in the deviatoric stress intensity, perhaps explaining why foreshocks and the main shock initiated close to the southern margin of the Tohoku-oki buttress. The megathrust may have been locking in the north, while unlocking was taking place in the south, defining a precursor to eventual catastrophic failure.

Strike-slip fault earthquakes are not observed because the accommodation structures are weak, and thus do not store strain energy. Such weakness is also a mechanical requirement to allow the abrupt transitions in tectonic mode that occur across them. Prior to the main shock, and during the aftershock sequence, the axis of principal compression north and south of the extensional channel was horizontal, trending orthogonal to the margin. Within the extensional channel, during the aftershock sequence, this principal compression axis is vertical. The abruptness of this transition requires the intervening zone of weakness be correspondingly narrow.

LANDWARD DIPPING NORMAL FAULTS IN THE SUBDUCTING PACIFIC SLAB

To better define the pattern of faulting in (and adjacent to) the Tohoku-oki extensional channel, the locations of the centroids and associated centroid moment tensors (CMTs) were recalculated (see Table DR2, footnote 1). This was done in order to improve the resolution on horizontal location and depth of the centroids reported in the Global CMT Project catalogue. We analyzed the broadband recordings by the F-net network, operated by National Research Institute for Earth Science and Disaster Resilience of Japan, selecting six high-quality stations with reasonable azimuthal coverage, noting that we had access only to on-shore stations. The CMT was computed for 84 events (Fig. 3), following methods as in Kikuchi and Kanamori (1986) and Zahradník et al. (2005).

Elementary seismograms were calculated for a 3-D set of grid nodes covering the earthquakes located in and around the Tohoku-oki extensional channel. Each elementary seismogram represents a basic mechanism, and a linear combination of these mechanisms can be used to represent an arbitrary moment tensor M:

$$M = \sum_m M_m a_m, \tag{1}$$

where M_m are the six components of a CMT and a_m are six corresponding coefficients. Using the relation between body force and ground motion, we can rewrite Eq.1 as follows:

$$D_i(x) = \sum_{m=1}^{6} \left(\frac{\partial\, G_{ij}(x;x_0)}{\partial (x_0)_{\hat{k}}}\, M_m \right) a_m \;\Rightarrow\; D = EA, \tag{2}$$

where D is the observed data (seismograms), G_{ij} are the elastodynamic Green's functions between the source (x_0) and receiver (x), and A is the vector with six coefficients to be determined.

A least-squares method was used to solve Eq. 2. One of the advantages of using this convention is that different constraints on the CMT components, such as deviatoric or pure double-couple inversion can simply be performed by choosing different subsets of CMTs in Eq. 1. The deviatoric CMT inversion assumed events that were pure double-couples, using the first five components as a basis. For each event, a spatiotemporal grid search over a selected number of nodes was performed, near the hypocenter, to find the CMT. The centroid time was searched by shifting the seismograms around the hypocenter time. A grid node location was then defined, and the time shift, which in combination provided the highest correlation between the observed and synthetic data as the optimum centroid location and time. The quality of all waveforms was checked manually and those with poor quality were removed prior to inversion.

The recalculation was made possible by a more detailed regional crustal structure model (Zhao et al., 1990) in comparison with the reference Earth model, PREM (Dziewoński and Anderson, 1981). This made it possible to predict ground motion down to 20 s, whereas the lowest period used in the Global CMT Project is 40 s. We could therefore constrain the depth for the crustal events confined within the top 25 km with more precision (as opposed to the Global CMT Project algorithm, in which the depth search stops at depths ≤12 km). Short period (<50 s) surface waves are sensitive to crustal structure and the short period body waves are sensitive to small-scale lateral heterogeneities in the mantle and crust. Using a low-pass filter to exclude periods shorter than 50 s, the Global CMT Project method avoids most effects of structural heterogeneity. This comes at a cost: at long periods, the ground motion due to dip-slip components trends toward zero for a shallow source. Therefore, the GCMT catalogue does not allow the depth parameter to be shallower than 12 km, and many of the earthquakes used in this study from the Global CMT Project database (Ekström et al., 2012; Nettles et al., 2011) had their centroid fixed at a depth of 12 km.

Lateral heterogeneity, even up to that present at the continental scale, can still affect waveforms filtered between 200 and 40 s, and thus influence the CMT solutions. Hejrani et al. (2017) have recently recalculated CMT solutions for 10 years of seismicity in Papua New Guinea and Solomon Islands using a 3-D crust and mantle model of Australia and its surroundings. The newly obtained continental-scale CMT solutions, in comparison with those in the standard Global CMT Project catalogue, have a significantly higher double-couple percentage and there is a considerably improved agreement in the inferred orientation of fault planes with the well-documented structural features that localized the earthquakes. This suggests that on local and regional scales (source-receiver distance <1000 km), a 1-D velocity model can be used to model data at 50–20 s. If the crust is not too heterogeneous, a range of 50–10 s would also work.

The model presented in Zhao et al. (1990) shows that a simple crustal structure exists from the slab interface to the Japanese mainland. This is the region that contains the earthquakes and stations used in this study. Our waveform modeling shows that the Zhao et al. (1990) model is detailed enough to allow higher frequencies to be successfully modeled. We have therefore computed Green's functions for a layered 0.1° spaced latitude-longitude grid, with a depth interval of 4 km. Best fit was determined based on waveform analysis (see below).

The relocated centroids (Fig. 4A) confirm the abrupt nature of the change in earthquake mode across the lineaments, and improved the definition of some orientation groups (Figs. 4B and 4C), lessening the scatter of slip lines and fault plane poles on the stereoplots. Significantly, this reveals well-defined orientation clusters, again with normal faults dipping ~60° landward. Further, the depth relocation allows a cross section (Fig. 4D) that reveals that the extensional channel is bounded at depth by the subducting Pacific Plate. In addition, the depth relocation of the cluster of normal faults at the trenchward-end of the extensional channel (Fig. 4) makes it evident that these earthquakes initiated within the down-going Pacific slab, implying that these faults cut and offset the megathrust, thus enhancing the role of gravity in driving motion of the overlying crust (McKenzie and Jackson, 2012). The slab faults also dip consistently landward, with slip vectors having the same trend as thrusts in the adjacent compressional buttresses.

GRAVITATIONAL COLLAPSE OF THE MARGIN ADJACENT TO A SLUMPING SLAB SHEET?

Our results open the question as to why lineament-bounded extensional channels mark segments of the East Japan megathrust with different geodynamic behavior to that of the adjacent compressional segments. This pattern implies that movement in the extensional channel was driven by seaward gravitational collapse of the Japanese crust, supporting the conclusions of previous authors (Cubas et al., 2013; McKenzie and

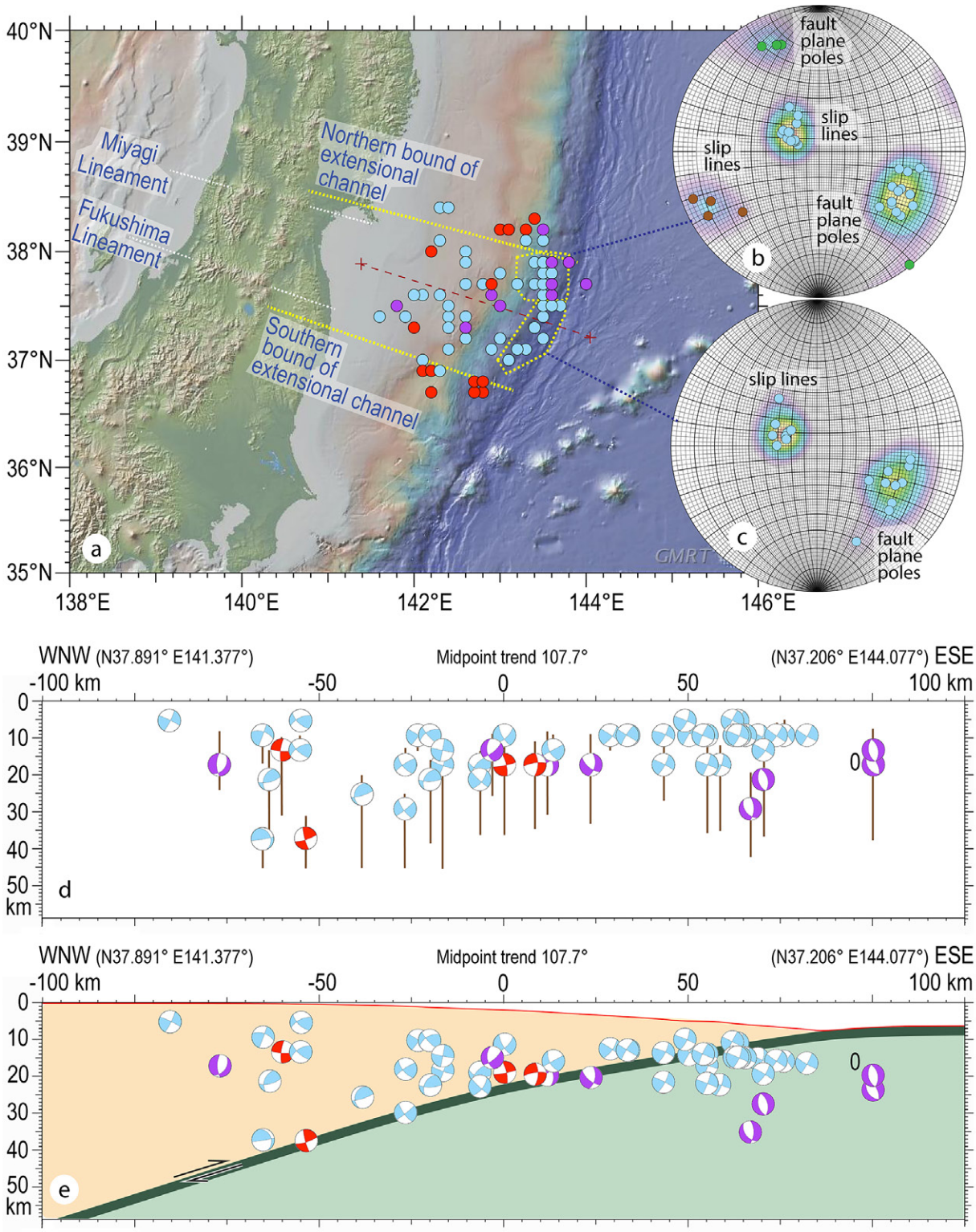

Figure 4. Relocated centroids on a map of the extensional aftershock channel (A) show normal faults closer inboard, with more accurate determination of the centroid moment tensors, and with scatter plots now showing the outermost normal faults consistently dipping landward (B, C). The cross sections (D) show centroids relative to the 1-D velocity model selected from (Zhao et al., 1990) with depth uncertainties as indicated. In (E), locations are corrected for increasing seawater depth. Thrusts are near the slab interface (red beachballs) with normal faults (light blue beachballs) scattered throughout the depth of the extensional channel. Slab normal faults beneath the margin began in the down-going Pacific plate, and ruptured upward through the megathrust. Left-lateral strike-slip faults (purple beachballs) formed in the down-going slab, parallel to the Median Tectonic Line. The plotted centroid depths do not lie in the center of the bars, because the bars represent the ranges of depths that are equally acceptable based on our chosen statistical criterion, namely that the variance reduction is greater than 90%.

Jackson, 2012; Scholz, 2014; Tsuji et al., 2013). Moreover, the implied switch in geodynamic mode represents abrupt transitions from mode-I to mode-II behavior on the megathrust, where: (*i*) mode-I involves the classic "push from behind" action (Scholz, 2014), and leads to crustal shortening; and (*ii*) mode-II requires movement on a weakened basal thrust, with motion associated with concomitant crustal extension in the overriding crust (Lister and Forster, 2018). In the latter circumstance, motion above the megathrust must be driven by gravity, at least during the aftershock sequence, and this requires the rupture to have offered negligible resistance.

Since the mode of deformation involves margin-orthogonal compression in the Tohoku-oki and Joban buttresses (i.e., mode-I megathrust behavior) to the north and south of the extensional channel, and changes to margin-orthogonal extension within it (i.e., to mode-II megathrust behavior), the relevant question is what weakened the basal megathrust between the two compressional buttresses. It is difficult to explain the margin segmentation without calling on the effects of a deep crustal structural control. The effects of deep-seated fluid activity could reduce effective stress on the overlying megathrust, and produce lubricating mineralogy as the megathrust slowly unlocked in the decade preceding catastrophic failure (Johnson et al., 2016; Mavrommatis et al., 2014, 2015; Yokota and Koketsu, 2015). The migration of fluids and magma upward along these deeper structures would explain why the volcanic lineaments developed in the first place (Tatsumi and Eggins, 1995). Fault splays from such deeper structures would also explain why the northern and southern boundaries of the extensional channel are offset ~15–20 km from the Miyagi and Fukushima Volcanic Lineaments.

An additional aspect needs to be considered, however. The cluster of normal faults at the trenchward-end of the extensional channel (Fig. 1E) appears to have initiated within the down-going Pacific slab, implying that these faults cut and offset the megathrust (McKenzie and Jackson, 2012), thus enhancing the role of gravity in driving motion of the overlying crust. The slab faults dip consistently landward, with slip vectors having the same trend as thrusts in the adjacent compressional buttresses. Although outer-rise normal faults are usually interpreted as the consequence of bending the slab as it enters the subduction zone, the consistent landward-dip of these structures suggests the existence of a slowly slumping slab sheet (Fig. 5), with a strike dimension comparable to the width of the extensional channel.

The stereoplots (Figs. 1 and 3) show that the headwall master faults dip landward, with the overall geometry comparable to that of the arrays of tilt-blocks due to margin orthogonal horizontal extension in the Basin and Range Province of the continental United States (Davis et al., 1986; Lister and Davis, 1989). Down-dip movement on these structures may connect (via a basal detachment) to the zone of seismicity that extends to ~150 km depth in the lowermost of the pair of seismic zones recognized in the down-going slab beneath East Japan. Data from CMTs can be interrogated to similarly allow inference as to the orientations of rupture fault planes and associated slip lines at these depths, allowing structural analysis in the double seismic zones. Interestingly the inferred orientations of the principal stress axes are consistent with a slumping slab sheet, particularly if Coulomb-Mohr failure is assumed at the "cold" top of the subducting slab, and ductile failure in its depths where the slab is dewatering (Peacock, 2001). Earthquakes in the double seismic zone have been shown to have gently dipping attitudes (e.g., Warren et al., 2007; Kita et al., 2010) with a geometry that is consistent with semi-brittle failure of a stretching slab-sheet with limited ductility.

Fault planes for intermediate depth earthquakes in the double seismic zone are never parallel to the locus of the double seismic zones (Fig. 6), implying that aseismic movement takes place both on the slab interface (where it couples to the weak asthenosphere) and at depth, where the lowermost of the doubled-planed seismic zones reflects material weakness. In this case, the behavior of the slumping slab-sheet is no different to what is observed at mesoscopic scale in most crustal-scale ductile shear zones. Figure 6 shows the geometry of the subhorizontal fault planes that can be inferred using CMT data, consistent with the analysis of Warren et al. (2007) and with the locus of high resolution relocated hypocenters (Kita et al., 2010). These data suggest that slip on both interfaces is aseismic, but that the slab sheet itself fails from time to time due to stretching as it slumps down the slab interface.

It should also be noted that the spatial coincidence between the extensional channel and the swarm of outer-rise normal fault earthquakes in the adjacent subducting Pacific slab suggests dynamic interactions between structures in the down-going slab with structures in the overriding Japanese lithosphere. The longevity of the volcanic lineaments implies that the dominant structural control might well have been exerted by mechanical properties of the overriding plate throughout the five million years during which volcanic activity has occurred in the observed lineaments (Tatsumi and Eggins, 1995). Mechanically, the implications of our observed juxtaposition of regions with distinctly opposing stress orientations is important, since it requires abrupt spatial switches from margin-orthogonal horizontal shortening, to margin-orthogonal horizontal extension. This increases the rate of deviatoric stress build-up on adjacent megathrust segments, which explains the repeated focusing of the onset of failure.

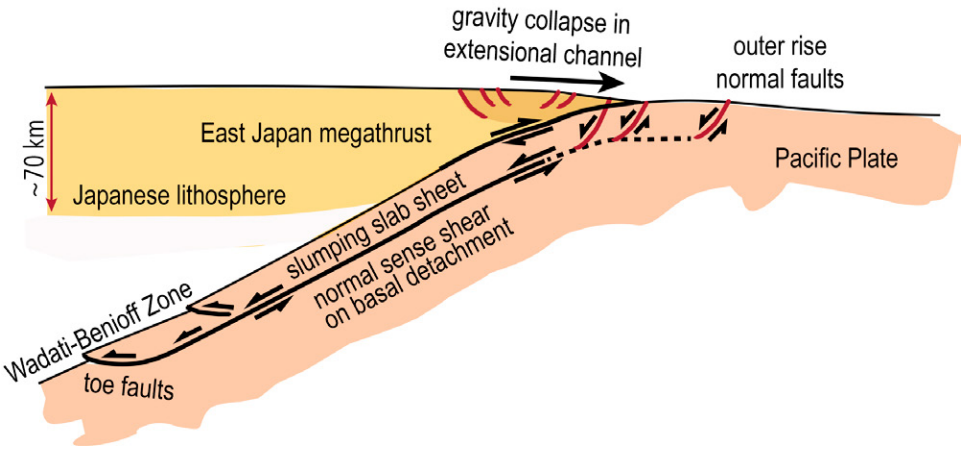

Figure 5. Interpretation of slab normal faults as marking the headwall faults of Basin and Range style extension, with displacement linking to the lowermost of the double seismic zones in the subducting Pacific Plate beneath Japan. Seismic activity in the double seismic zone may delimit the base of a detachment-floored mega-slump.

In any case, the extensional Tohoku-oki earthquake channel at surface levels is limited in its extent, so it cannot be explained by general horizontal extension as would be possible if there was subduction roll-back. A more local explanation is required. We suggest that movement on outer-rise normal faults created a gravitational potential well, and this drove seaward flow of the Japanese crust in the adjacent extensional channel (cf. McKenzie and Jackson, 2012). This does require reduced basal friction on the megathrust to allow this segment to act in this way. Perhaps the slab dewatering from the double seismic zone below lubricated the fault plane (through the development of soft mineralogy) or lenses of pressured pore fluid may have reduced the effective stress in the extensional segment of the megathrust, thus maintaining its weakened state.

DISCUSSION

To understand why the segment boundaries have focused the onset of the largest earthquakes in the past four decades in East Japan, we need to bring geology into the equation, at the scale involved in modeling subduction zone interactions (Bassett et al., 2016; Freed et al., 2017; Hashima and Sato, 2017; Hu et al., 2016). Geological architecture responds to loading just like any man-made construction. A failure that leads to catastrophic release of energy in an overloaded structure can be triggered by a stress concentration associated with movement on a simple weakness. Irrespective of the magnitude of the displacements involved, such structures are often expressed as geomorphic features (e.g., the volcanic lineaments). Less obvious seismotectonic lineaments coincide with the boundaries of the extensional earthquake channel, even though these delineate fundamental structural switches in behavior and act as controlling features that determine the earthquake geology. If there are faults associated with these bounding seismotectonic lineaments, they outcrop in valleys adjacent to the volcanic lineaments.

A key finding is that the sense of movement on the southern boundary of the Tohoku-oki buttress reversed prior to the catastrophic earthquake of 11 March 2011. Movement across the southern boundary of the Tohoku-oki buttress involved left-lateral strike-slip displacement in the decade prior to the 2011 Great Earthquake, but the sense of relative motion became right-lateral as the buttress accelerated seaward in the days prior to the main shock. Precise monitoring across the lineaments is thus essential, for this change in movement pattern within the geological architecture can be interpreted as a pre-yield phenomenon, implying that its early detection may have been of some use in seismic hazard assessment. Perhaps other lineaments (and associated compressional buttresses) deserve closer attention, e.g., in the Sanriku region (Nomura et al., 2017; Ye et al., 2012). The Sanriku Lineament marks the southern bound of a compressional buttress, with an extensional earthquake channel to its south. It is therefore directly analogous to the structure that localized onset of the 2011 Great Earthquake. Large tsunamis (Tanioka and Sataka, 1996) related to normal faults (Uchida et al., 2016a, 2016b) imply the possible existence of a second slab sheet slump seaward of the Sanriku extensional earthquake channel.

A key issue thus becomes how to determine which aspects of the geological architecture deserve more focus. A key consequence of the 2011 Great Earthquake is that it occasioned a major release of stored elastic energy, and it may take decades or centuries to once again build up deviatoric stress to critical levels on these segments (Nomura et al., 2017). So, while the southern boundary of the Tohoku-oki buttress localized the onset of mechanical failure for the main shock of the 2011 Great

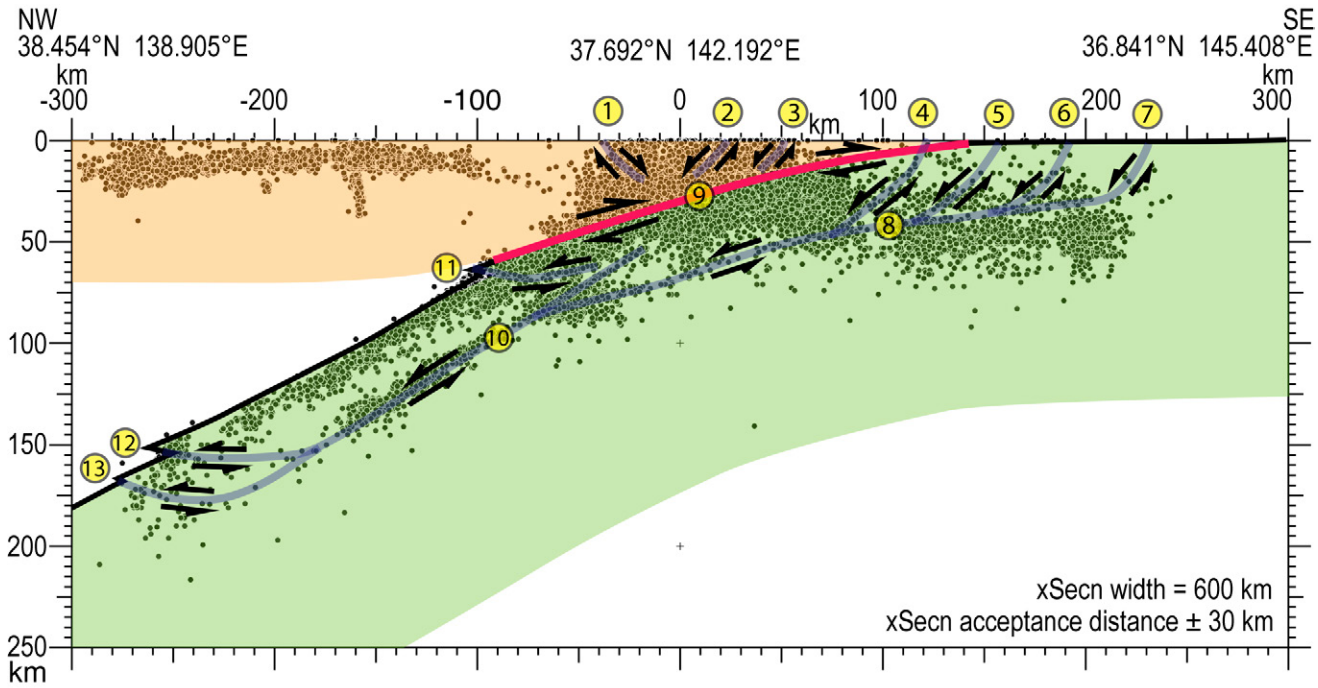

Figure 6. Structural interpretation of a slab-sheet slump superimposed an image of hypocenters adjacent to the cross-section using data from the International Seismological Centre website: Bulletin of the International Seismological Center, 2015, Thatcham, UK, http://www.isc.ac.uk/iscbulletin/. Hypocenter data are taken ipso facto with no attempt at relocation. Normal faults (1, 2, 3) are from the extensional channel, above the megathrust (9). Normal faults (4, 5) are slab faults that cut the megathrust, while normal faults (5, 6, 7) are slab faults further seaward in the slab beneath the outer rise. It is supposed that motion on these faults transfers into movement on a basal detachment (8) that transfers into a detachment (10) parallel to the lowermost of the paired seismic zones observed in the slab beneath Japan. The relative motion of the slumping slab sheet is accommodated by gently dipping toe thrusts in the Benioff zone.

Earthquake, and the initiation of several past large earthquakes on the East Japan Megathrust, including the 2005 M_w ~7.2 Miyagi Earthquake, this bounding lineament may not exhibit stress concentration for a considerable time into the future. This suggests that other lineaments now deserve more attention. The most recent large earthquake offshore East Japan initiated close to the prolongation of the Fukushima Lineament (Fig. 2), for example.

Routine detection of precursor movements in the geological architecture would advance the science of earthquake forecasting (Barbot et al., 2012; Hori et al., 2014; Kaneko et al., 2010; Stuart, 1988). The Japanese Median Tectonic Line is already recognized (Bassett et al., 2016; Ikeda et al., 2009) as a focusing structure, but this is for strike-slip earthquakes. The prolongations of the lineaments of East Japan may be more significant since these attest to the existence of natural weaknesses that repeatedly focus the onset of megathrust failure. Precise geodetic monitoring of relative displacement across the prolongations of such structures is thus warranted in order that continuous signals might inform policy and response.

There are numerous cautionary tales in respect to the "science" of earthquake forecasting. Many argue that it should not be attempted. Risk analysis based on precursor (?) movements in the geological architecture will require the light of decades in order to develop quantitative constraints. Nevertheless, our broader investigation implies that improved accounting for structural controls might well have allowed a few days warning in advance of the March 2011 earthquake, at least providing the opportunity of taking precautionary measures in respect to the operation of major infrastructure, e.g., the Fukushima nuclear reactor. To recognize focused relative displacements on structures within the geological architecture, we recommend increased attention to the geodetic network. There are solutions that would allow monitoring of the dominant lineaments for the types of shuffling movements recognized in this paper, thus providing continuous signals to inform policy and response in this seismically active region.

CONCLUSION

Structural weaknesses localize the onset of catastrophic failure in any loaded architecture. Our study has demonstrated this relation in detail for the East Japan Megathrust. The visible volcanic lineaments on land are parallel to seismotectonic lineaments. The associated fault structures must be weak, since they are not seismogenic. Mechanically, this allows them to separate segments of the megathrust above which the crust exhibits distinctly different geodynamic behavior, evidenced by the contrasting seismotectonic response of compressional buttresses and intervening extensional earthquake channels. For a decade prior to the 2011 Great Earthquake relative to the Tohoku-oki buttress, the extensional earthquake margin segment to its south accelerated seaward, potentially reflecting an unlocking segment of the megathrust. Three days before the Tohoku-oki Great Earthquake, the Tohoku-oki buttress began to accelerate seaward. The sense of relative movement across the bounding seismotectonic lineament reversed. This shuffling motion on an accommodating structure that focuses margin segmentation may be an intrinsic part of the seismic cycle, and the reversal of shear-sense across the southern boundary of the Tohoku-oki buttress was a precursor signal that reflected the onset of catastrophic failure.

ACKNOWLEDGMENTS

The research reported here was supported by the Satellites, Seismometers and Mass Spectrometers initiative, a joint venture between the Structure Tectonics team and the Geodesy and Geodynamics team in the Earth Dynamics Group, and the Seismology and Mathematical Geophysics Group at the Research School of Earth Sciences. Additional support derived from Australian Research Council Discovery Project DP120103554 and Linkage Project LP130100134. EJR acknowledges Australian Laureate Fellowship FL120100050. We would like to thank Nick Rawlinson and one anonymous reviewer who considerably improved the manuscript through thorough, systematic, and careful review.

REFERENCES CITED

Barbot, S., Lapusta, N., and Avouac, J.P., 2012, Under the hood of the earthquake machine: Toward predictive modeling of the seismic cycle: Science, v. 336, no. 6082, p. 707–710, https://doi.org/10.1126/science.1218796.

Bassett, D., Sandwell, D.T., Fialko, Y., and Watts, A.B., 2016, Upper-plate controls on co-seismic slip in the 2011 magnitude 9.0 Tohoku-oki earthquake: Nature, v. 531, no. 7592, p. 92–96, https://doi.org/10.1038/nature16945.

Cubas, N., Avouac, J.P., Leroy, Y.M., and Pons, A., 2013, Low friction along the high slip patch of the 2011 M_w 9.0 Tohoku-Oki earthquake required from the wedge structure and extensional splay faults: Geophysical Research Letters, v. 40, no. 16, p. 4231–4237, https://doi.org/10.1002/grl.50682.

Davis, G.A., Lister, G.S., and Reynolds, S.J., 1986, Structural evolution of the Whipple and South mountains shear zones, southwestern United States: Geology, v. 14, no. 1, p. 7–10, https://doi.org/10.1130/0091-7613(1986)14<7:SEOTWA>2.0.CO;2.

Dziewoński, A.M., and Anderson, D.L., 1981, Preliminary reference Earth model: Physics of the Earth and Planetary Interiors, v. 25, no. 4, p. 297–356, https://doi.org/10.1016/0031-9201(81)90046-7.

Ekström, G., Nettles, M., and Dziewoński, A.M., 2012, The global CMT project 2004–2010: Centroid-moment tensors for 13,017 earthquakes: Physics of the Earth and Planetary Interiors, v. 200–201, p. 1–9, https://doi.org/10.1016/j.pepi.2012.04.002.

Freed, A.M., Hashima, A., Becker, T.W., Okaya, D.A., Sato, H., and Hatanaka, Y., 2017, Resolving depth-dependent subduction zone viscosity and afterslip from postseismic displacements following the 2011 Tohoku-oki, Japan earthquake: Earth and Planetary Science Letters, v. 459, p. 279–290, https://doi.org/10.1016/j.epsl.2016.11.040.

Ghimire, S., and Kasahara, M., 2009, Spatial variation in seismotectonics and stress conditions across the Kurile and Japan trenches inferred from the analysis of focal mechanism data in Hokkaido, northern Japan: Journal of Geodynamics, v. 47, p. 153–166, https://doi.org/10.1016/j.jog.2008.07.007.

Hasegawa, A., and Yoshida, K., 2015, Preceding seismic activity and slow slip events in the source area of the 2011 Mw 9.0 Tohoku-Oki earthquake: A review: Geoscience Letters, v. 2, no. 1, https://doi.org/10.1186/s40562-015-0025-0.

Hashima, A., and Sato, T., 2017, A megathrust earthquake cycle model for Northeast Japan: Bridging the mismatch between geological uplift and geodetic subsidence: Earth, Planets, and Space, v. 69, no. 1, https://doi.org/10.1186/s40623-017-0606-6.

Hejrani, B.R., Hatami, M., and Mousavi, S., 2010, Fault-plane Identification by a Geometrical Method—Application to Moderate Earthquake Mw 5.1 Kerman, Iran, Proceedings, 72nd European Association of Geoscientists and Engineers Conference and Exhibition incorporating SPE EUROPEC 2010, Barcelona, Spain, 14-17 June 2010: European Association of Geoscientists and Engineers, https://doi.org/10.3997/2214-4609.201401311.

Hejrani, B., Tkalčić, H., and Fichtner, A., 2017, Centroid moment tensor catalogue using 3D continental scale Earth model: Application to earthquakes in Papua New Guinea and the Solomon Islands: Journal of Geophysical Research, v. 122, p. 5517–5543, https://doi.org/10.1002/2017JB014230.

Hori, T., Hyodo, M., Miyazaki, S.I., and Kaneda, Y., 2014, Numerical forecasting of the time interval between successive M8 earthquakes along the Nankai Trough, southwest Japan, using ocean bottom cable network data: Marine Geophysical Researches, v. 35, no. 3, p. 285–294, https://doi.org/10.1007/s11001-014-9226-8.

Hu, Y., Bürgmann, R., Uchida, N., Banerjee, P., and Freymueller, J.T., 2016, Stress-driven relaxation of heterogeneous upper mantle and time-dependent afterslip following the 2011 Tohoku earthquake: Journal of Geophysical Research, Solid Earth, v. 121, no. 1, p. 385–411.

Ikeda, M., Toda, S., Kobayashi, S., Ohno, Y., Nishizaka, N., and Ohno, I., 2009, Tectonic model and fault segmentation of the Median Tectonic Line active fault system on Shikoku, Japan: Tectonics, v. 28, no. 5, https://doi.org/10.1029/2008TC002349.

Ikuta, R., Satomura, M., Fujita, A., Shimada, S., and Ando, M., 2012, A small persistent locked area associated with the 2011 M_w 9.0 Tohoku-Oki earthquake, deduced from GPS data: Journal of Geophysical Research, Solid Earth, v. 117, no. B11, http://10.1029/2012JB009335.

Jackson, J.A., 1987, Active normal faulting and crustal extension, *in* Coward, M.P., Dewey, J.F., and Hancock, P.L., eds., Continental Extensional Tectonics: Geological Society of London, Special Publications, v. 28, no. 1, p. 3–17, https://doi.org/10.1144/GSL.SP.1987.028.01.02.

Johnson, K.M., Mavrommatis, A., and Segall, P., 2016, Small interseismic asperities and widespread aseismic creep on the northern Japan subduction interface: Geophysical Research Letters, v. 43, no. 1, p. 135–143, https://doi.org/10.1002/2015GL066707.

Kamiyama, M., Sugito, M., Kuse, M., Schekotov, A., and Hayakawa, M., 2016, On the precursors to the 2011 Tohoku earthquake: Crustal movements and electromagnetic signatures: Geomatics, Natural Hazards & Risk, v. 7, no. 2, p. 471–492, https://doi.org/10.1080/19475705.2014.937773.

Kanamori, H., and Press, F., 1970, How Thick Is the Lithosphere?: Nature, v. 226, p. 330–331, https://doi.org/10.1038/226330a0.

Kaneko, Y., Avouac, J.-P., and Lapusta, N., 2010, Towards inferring earthquake patterns from geodetic observations of interseismic coupling: Nature Geoscience, v. 3, no. 5, p. 363–369, https://doi.org/10.1038/ngeo843.

Kato, A., Obara, K., Igarashi, T., Tsuruoka, H., Nakagawa, S., and Hirata, N., 2012, Propagation of slow slip leading up to the 2011 M_w 9.0 Tohoku-Oki earthquake: Science, v. 335, no. 6069, p. 705–708, https://doi.org/10.1126/science.1215141.

Kikuchi, M., and Kanamori, H., 1986, Inversion of complex body waves—II: Physics of the Earth and Planetary Interiors, v. 43, no. 3, p. 205–222, https://doi.org/10.1016/0031-9201(86)90048-8.

Kita, S., Okada, T., Hasegawa, A., Nakajima, J., and Matsuzawa, T., 2010, Existence of interplane earthquakes and neutral stress boundary between the upper and lower planes of the double seismic zone beneath Tohoku and Hokkaido, Northeastern Japan: Tectonophysics, v. 496, p. 68–82, https://doi.org/10.1016/j.tecto.2010.10.010.

Kumamoto, T., Tsukada, M., and Fujita, M., 2016, Multivariate statistical analysis for seismotectonic provinces using earthquake, active fault, and crustal structure datasets, *in* Kamae, K., ed., Earthquakes, Tsunamis and Nuclear Risks: Tokyo, Springer, https://doi.org/10.1007/978-4-431-55822-4_2.

Kyriakopoulos, C., Masterlark, T., Stramondo, S., Chini, M., and Bignami, C., 2013, Coseismic slip distribution for the M_w 9 2011 Tohoku-Oki earthquake derived from 3-D FE modeling: Journal of Geophysical Research, Solid Earth, v. 118, p. 3837–3847, https://doi.org/10.1002/jgrb.50265.

Lister, G.S., and Davis, G.A., 1989, The origin of metamorphic core complexes and detachment faults formed during Tertiary continental extension in the northern Colorado River region, U.S.A: Journal of Structural Geology, v. 11, p. 65–94, https://doi.org/10.1016/0191-8141(89)90036-9.

Lister, G.S., and Forster, M.A., 2018, Structural geology and the seismotectonics of the 2004 Great Sumatran Earthquake: Tectonics, https://doi.org/10.1002/2017TC004708.

Lister, G., Kennett, B., Richards, S., and Forster, M., 2008, Boudinage of a stretching slablet implicated in earthquakes beneath the Hindu Kush: Nature Geoscience, v. 1, no. 3, p. 196–201, https://doi.org/10.1038/ngeo132.

Lister, G.S., Tkalčić, H., McClusky, S., and Forster, M.A., 2014, Skewed orientation groups in scatter plots of earthquake fault plane solutions: Implications for extensional geometry at oceanic spreading centers: Journal of Geophysical Research, Solid Earth, v. 119, no. 3, p. 2055–2067, https://doi.org/10.1002/2013JB010706.

Loveless, J.P., and Meade, B.J., 2016, Two decades of spatiotemporal variations in subduction zone coupling offshore Japan: Earth and Planetary Science Letters, v. 436, p. 19–30, https://doi.org/10.1016/j.epsl.2015.12.033.

Mavrommatis, A.P., Segall, P., and Johnson, K.M., 2014, A decadal-scale deformation transient prior to the 2011 M_w 9.0 Tohoku-oki earthquake: Geophysical Research Letters, v. 41, no. 13, p. 4486–4494, https://doi.org/10.1002/2014GL060139.

Mavrommatis, A.P., Segall, P., Uchida, N., and Johnson, K.M., 2015, Long-term acceleration of aseismic slip preceding the M_w 9 Tohoku-oki earthquake: Constraints from repeating earthquakes: Geophysical Research Letters, v. 42, no. 22, p. 9717–9725, https://doi.org/10.1002/2015GL066069.

McKenzie, D., and Jackson, J., 2012, Tsunami earthquake generation by the release of gravitational potential energy: Earth and Planetary Science Letters, v. 345–348, p. 1–8, https://doi.org/10.1016/j.epsl.2012.06.036.

Nakajima, J., Hirose, F., and Hasegawa, A., 2009, Seismotectonics beneath the Tokyo metropolitan area, Japan: Effect of slab-slab contact and overlap on seismicity: Journal of Geophysical Research, v. 114, B08309, https://doi.org/10.1029/2008JB006101.

Nettles, M., Ekström, G., and Koss, H.C., 2011, Centroid-moment-tensor analysis of the 2011 off the Pacific coast of Tohoku Earthquake and its larger foreshocks and aftershocks: Earth, Planets, and Space, v. 63, no. 7, p. 519–523, https://doi.org/10.5047/eps.2011.06.009.

Nomura, S., Ogata, Y., Uchida, N., and Matsu'ura, M., 2017, Spatiotemporal variations of interplate slip rates in northeast Japan inverted from recurrence intervals of repeating earthquakes: Geophysical Journal International, v. 208, no. 1, p. 468–481, https://doi.org/10.1093/gji/ggw395.

Ozawa, S., Nishimura, T., Munekane, H., Suito, H., Kobayashi, T., Tobita, M., and Imakiire, T., 2012, Preceding, coseismic, and postseismic slips of the 2011 Tohoku earthquake, Japan: Journal of Geophysical Research, Solid Earth, v. 117, no. B7, https://doi.org/10.1029/2011JB009120.

Peacock, S.M., 2001, Are the lower planes of double seismic zones caused by serpentine dehydration in subducting oceanic mantle?: Geology, v. 29, p. 299–302, https://doi.org/10.1130/0091-7613(2001)029<0299:ATLPOD>2.0.CO;2.

Perfettini, H., and Avouac, J.P., 2014, The seismic cycle in the area of the 2011 M_w 9.0 Tohoku-Oki earthquake: Journal of Geophysical Research, v. 119, no. 5, p. 4469–4515, https://doi.org/10.1002/2013JB010697.

Ryan, W.B.F., Carbotte, S.M., Coplan, J.O., O'Hara, S., Melkonian, A., Arko, R., Weissel, R.A., Ferrini, V., Goodwillie, A., Nitsche, F., Bonczkowski, J., and Zemsky, R., 2009, Global Multi-Resolution Topography synthesis: Geochemistry, Geophysics, Geosystems, v. 10, no. 3, https://doi.org/10.1029/2008GC002332.

Sato, T., Hiratsuka, S., and Mori, J., 2013, Precursory seismic activity surrounding the high-slip patches of the 2011 M_w 9.0 Tohoku-Oki earthquake: Bulletin of the Seismological Society of America, v. 103, no. 6, p. 3104–3114, https://doi.org/10.1785/0120130042.

Scholz, C.H., 2014, The rupture mode of the shallow large-slip surge of the Tohoku-Oki earthquake: Bulletin of the Seismological Society of America, v. 104, no. 5, p. 2627–2631, https://doi.org/10.1785/0120140130.

Stuart, W.D., 1988, Forecast model for great earthquakes at the Nankai Trough subduction zone: Pure and Applied Geophysics, v. 126, no. 2–4, p. 619–641, https://doi.org/10.1007/BF00879012.

Tanioka, Y., and Sataka, K., 1996, Fault parameters of the 1896 Sanriku tsunami earthquake estimated from Tsunami Numerical Modeling: Geophysical Research Letters, v. 23, no. 13, p. 1549–1552, https://doi.org/10.1029/96GL01479.

Tatsumi, Y., and Eggins, S., 1995, Subduction Zone Magmatism: Cambridge, Blackwell, Frontiers in Earth Sciences, 211 p.

Triyoso, W., and Shimazaki, K., 2012, Testing various seismic potential models for hazard estimation against a historical earthquake catalog in Japan: Earth, Planets, and Space, v. 64, no. 8, p. 673–681, https://doi.org/10.5047/eps.2011.02.003.

Tsuji, T., Kawamura, K., Kanamatsu, T., Kasaya, T., Fujikura, K., Ito, Y., Tsuru, T., and Kinoshita, M., 2013, Extension of continental crust by anelastic deformation during the 2011 Tohoku-oki earthquake: The role of extensional faulting in the generation of a great tsunami: Earth and Planetary Science Letters, v. 364, p. 44–58, https://doi.org/10.1016/j.epsl.2012.12.038.

Uchida, N., Iinuma, T., Nadeau, R.M., Burgmann, R., and Hino, R., 2016a, Periodic slow slip triggers megathrust zone earthquakes in northeastern Japan: Science, v. 351, no. 6272, p. 488–492, https://doi.org/10.1126/science.aad3108.

Uchida, N., Kirby, S.H., Umino, N., Hino, R., and Kazakami, T., 2016b, The great 1933 Sanriku-oki earthquake: Reappraisal of the main shock and its aftershocks and implications for its tsunami using regional tsunami and seismic data: Geophysical Journal International, v. 206, no. 3, p. 1619–1633, https://doi.org/10.1093/gji/ggw234.

Warren, L.M., Hughes, A.N., and Silver, P.G., 2007, Earthquake mechanics and deformation in the Tonga-Kermadec subduction zone from fault plane orientations of intermediate- and deep-focus earthquakes: Journal of Geophysical Research, v. 112, https://doi.org/10.1029/2006JB004677.

Ye, L., Lay, T., and Kanamori, H., 2012, The Sanriku-Oki low-seismicity region on the northern margin of the great 2011 Tohoku-Oki earthquake rupture: Journal of Geophysical Research. Solid Earth, v. 117, no. B2, https://doi.org/10.1029/2011JB008847.

Yokota, Y., and Koketsu, K., 2015, A very long-term transient event preceding the 2011 Tohoku earthquake: Nature Communications, v. 6, p. 5934, https://doi.org/10.1038/ncomms6934.

Zahradník, J., Serpetsidaki, A., Sokos, E., and Tselentis, G.A., 2005, Iterative deconvolution of regional waveforms and a double-event interpretation of the 2003 Lefkada earthquake, Greece: Bulletin of the Seismological Society of America, v. 95, no. 1, p. 159–172, https://doi.org/10.1785/0120040035.

Zahradník, J., Gallovič, F., Sokos, E., Serpetsidaki, A., and Tselentis, G.-A., 2008, Quick fault-plane identification by a geometrical method: Application to the M_w 6.2 Leonidio earthquake, January 6, 2008, Greece: Seismological Research Letters, v. 79, p. 653–662, https://doi.org/10.1785/gssrl.79.5.653.

Zhao, D., Horiuchi, S., and Hasegawa, A., 1990, 3-D seismic velocity structure of the crust and the uppermost mantle in the northeastern Japan Arc: Tectonophysics, v. 181, no. 1–4, p. 135–149, https://doi.org/10.1016/0040-1951(90)90013-X.

Zhao, D., Huang, Z., Umino, N., Hasegawa, A., and Kanamori, H., 2011, Structural heterogeneity in the megathrust zone and mechanism of the 2011 Tohoku-oki earthquake (M_w 9.0): Geophysical Research Letters, v. 38, no. 17, https://doi.org/10.1029/2011GL048408.

MANUSCRIPT RECEIVED 9 JULY 2017
REVISED MANUSCRIPT RECEIVED 20 FEBRUARY 2018
MANUSCRIPT ACCEPTED 3 APRIL 2018